Polymer assisted deposition

3 AUTHORS, INCLUDING:

Thomas Mark Mccleskey
Los Alamos National Laboratory
122 PUBLICATIONS **2,134** CITATIONS

SEE PROFILE

Quanxi Jia
Los Alamos National Laboratory
564 PUBLICATIONS **10,566** CITATIONS

SEE PROFILE

Polymer assisted deposition

Anthony K. Burrell,* T. Mark McCleskey and Q. X. Jia

Polymer assisted deposition (PAD) is a chemical solution route to high quality thin films of metal oxides. This technique employs metal ions coordinated to polymers as the film precursor. The use of polymer bound metals has several advantages. The polymer controls the viscosity and binds metal ions, resulting in a homogeneous distribution of metal precursors in the solution and the formation of uniform metal oxide films. The nature of the metal oxide deposition is dominated by bottom-up growth, leading to ready formation of crack-free epitaxial metal oxides and the ability to coat nanofeatured substrates in a conformal fashion.

Introduction

The diverse and application rich properties of metal oxide thin films such as high-temperature superconductivity, ferroelectricity, ferromagnetism, piezoelectricity and semiconductivity, continue to receive significant attention. Metal oxide films are conventionally grown by physical and chemical vapour deposition.[1,2] All growth methods have their advantages and disadvantages. Vacuum techniques provide high quality materials and excellent thickness control, but production rates are restricted by the cost of scaling vacuum systems. Chemical-solution depositions such as sol–gel are more cost-effectively scaled and since vacuum is not required oxygen stoichiometry is easy to maintain.[3] However, chemical-solution techniques are limited in that not all types of metal oxides can be deposited and the control of stoichiometry is not always possible owing to differences in chemical reactivity among the metals. In addition, the formation of high density films employing chemical-solution techniques is often difficult.

Chemical solution methods

Sol–gel processing is perhaps the most well known and extensively studied method for chemical solution deposition of thin films and as such has received much attention.[4–6] However, other solution techniques have been developed and provide viable alternatives to the physical deposition methods.[7]

Sol–gel

In general, the sol–gel process involves the transition of a system from a liquid "sol" (mostly colloidal) into a solid "gel" phase. The starting materials used in the preparation of the "sol" are usually reactive inorganic metal salts or metal organic compounds such as metal alkoxides. In a typical sol–gel process, the precursor is subjected to a series of hydrolysis and polymerization reactions to form a colloidal suspension, or a "sol". Thermal treatment of the sol results in

Materials Chemistry, Materials Physics and Applications, Los Alamos National Laboratory, Los Alamos, NM 87545, USA. E-mail: Burrell@LANL.GOV; Fax: 1 505 667 9905; Tel: 01 505 667 9342

the complete loss of the alkoxides as alcohol and formation of the metal oxide.

Chemical bath techniques (CBT)

This is perhaps the oldest known chemical method for the formation of thin films, dating back to 1884 when PbS was deposited using thiourea.[8] This technique usually involves the simple immersion of a substrate into a solution containing both a metal salt and a chalcogenide precursor. As such it has generally been dominated by the formation of sulfides and selenide films.[9] However, in recent years considerable work on the formation of oxide films has been carried out.[7] CBT require that the product of the metal ion concentrations and the chalcogenide must exceed the solubility product of the desired product, thus the maximum obtainable thickness is limited by the supply of the reactants in solution. Control of film thickness, composition and density require complex control of the solution composition, pH and temperature.

Successive ion layer absorption and reaction (SILAR)

SILAR was developed in the early 1980s as an alternative method for the formation of metal sulfide[10] and oxide films.[11] SILAR employs immersion of the substrate in alternating aqueous solutions of metal cations and chalcogenide salts.[12] This results in layer-by-layer build up of the individual atomic layers of the material of the order of 1.3 Å per cycle. This process, while very laborious, can be automated and high quality films can be obtained.

Liquid phase deposition (LPD)

LPD employs metal fluorides, which are hydrolysed in water by boric acid, as precursors to metal oxide thin films. The boric acid or aluminium acts as a fluoride scavenger. Compared to the formation of oxide films by CBD, the use of the fluoride scavenger allows for better control of the hydrolysis reaction and of the solution's supersaturation. The general scheme for the reactions is given by eqn (1) and (2).
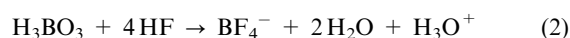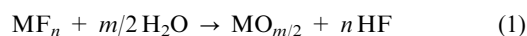
$$MF_n + m/2\,H_2O \rightarrow MO_{m/2} + n\,HF \qquad (1)$$

$$H_3BO_3 + 4\,HF \rightarrow BF_4^- + 2\,H_2O + H_3O^+ \qquad (2)$$

This process is exclusively employed for the formation of oxide films and has been used to produce a wide range of metal oxide materials.[7] In particular, LPD silica has been widely promoted for use in metal oxide semiconductor technologies and other applications such as solar cells.[13]

Overall, one of the greatest challenges in solution-based processes of complex metal oxide films, has been to produce high-quality films with desired chemical composition. Several years ago we began employing metal complexes of the polymer poly(ethyleneimine) (PEI) as a route to metal oxide film deposition.[14] Polymer assisted deposition (PAD), has the traditional advantages of chemical-solution deposition systems and has the added feature of producing high quality films comparable to physical vapour deposition (PVD). Binding the metals directly to the polymer has several advantages including homogeneous distribution of metal precursors, and sequestering the metal until the polymer is decomposed. Sequestering the metal eliminates metal oxide formation in solution and results in a true bottom-up film formation that yields crack-free, epitaxial metal oxides. The precursors are air- and water-stable and the metal polymer can be spun, dip or spray coated on to the substrate. Thermal decomposition of the metal polymer results in the formation of high density, even epitaxial, films of metal oxides.

Metal polymer solutions

The key to PAD is the inherent stability of the metal polymer solutions. The simplest view of the metal polymer interactions is the formation of covalent complexes between the lone pairs on the nitrogen atoms and the metal cation. This classic Werner-type chemistry is clearly the simplest method for the formation of first-row transition metals, using nitrates, acetates or chlorides. One of the key features in the formation of the complexes is the use of Amicon® filtration to remove non-coordinated species.

The first-row transition metals bind well to the simple PEI polymer, presumably in a manner as shown in Fig. 1 (left). Other hard metals such as titanium require PEI functionalised with carboxylic acids to provide a stable coordination environment (Fig. 1, right). Another method for binding metals utilises the ability of protonated PEI to coordinate anionic metal complexes as shown in Fig. 2 (right). While these options provide for the formation of a wide range of metal bound polymers we discovered that ethylenediaminetetra-acetic acid (EDTA) complexes in combination with PEI work
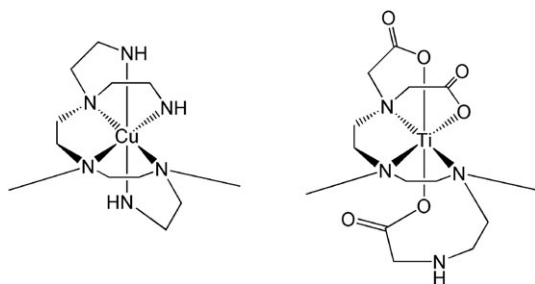

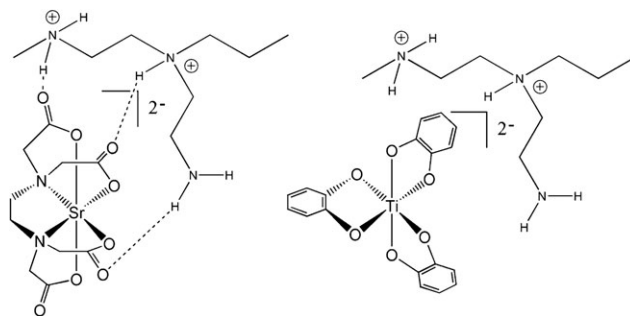Fig. 1 Putative structures of PEI and carboxylic acid functionalised PEI metal complexes.

Fig. 2 Putative structures of PEI binding EDTA complexes by hydrogen bonding and electrostatic binding.

as well as functionalised PEI in most cases. The major advantage of the EDTA route is that EDTA forms stable complexes with almost all metals. The EDTA complexes bind to the PEI *via* a combination of hydrogen bonding and electrostatic attraction as seen in Fig. 2 (left). This hydrogen bonding is sufficiently stable that the Amicon® filtration can also be used to purify these polymers.

Using either pure PEI or PEI–EDTA we have been able to produce metal polymers of over 45 different elements. In general, it is also possible to mix polymers in any ratio desired. These solutions can remain stable for months even when multiple metals are used.

Once the metal polymers have been prepared their viscosity can be adjusted by the simple removal of water under vacuum or by dilution with deionised water. The solution can then be applied onto a substrate through either spin-coating or dipping.

Thermal depolymerization

Perhaps the most important aspect of the PAD process is the thermal removal of the polymer. The polymer acts to protect the metals from premature condensation and enables the formation of homogeneous films by allowing complete mixing of the metals before film formation. Initially we considered this to be a combustion process.[14] This is not the case. The polymer does not undergo combustion as it is removed at temperatures > 350 °C. Instead it undergoes thermal depolymerisation back to $NH_2CH=CH_2$. The EDTA decomposes to acetic acid, formic acid and ethylenediamine.[15] These non-combustion processes result in extremely clean metal oxide films even in inert or hydrogen atmospheres. In fact, PEI can be completely depolymerised in a hydrogen atmosphere with no coke formation. During the thermal decomposition of the polymer, the film is effectively molten providing for a very effective mixing of the metal cations. The fact that the metals remain homogeneously mixed until the polymer is removed allows for the formation of thermodynamically unstable materials based on templating from the substrate structure. We recently prepared the first reported example of the epitaxial growth of $CuAlO_2$ films, a material particularly prone to phase separation. The X-ray data for the epitaxial $CuAlO_2$ films are shown in Fig. 3.[16]
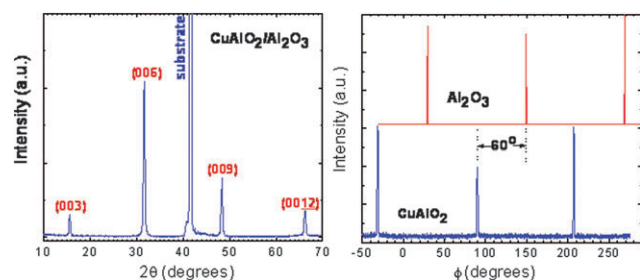
Fig. 3 XRD patterns of the CuAlO$_2$ film on a c-plane sapphire substrate. Left is the θ–2θ scan and right are the ϕ-scans from (012) reflections of both the substrate and the film.

Epitaxial metal oxides

Simple metal oxide films based on a single metal such as Eu$_2$O$_3$ can be prepared using the europium polymer prepared using the acid-functionalised PEI.[17] The resulting solution was spin coated on LaAlO$_3$ (LAO) substrates and thermally annealed in oxygen. The polymer was decomposed by initially heating slowly to 500 °C. This was followed by heating at 1000–1200 °C for 1 h. The thicknesses of the films can be controlled by adjusting the viscosity of the solution and/or the rate of spin coating. The films were generally on the order of 20–40 nm.

X-Ray diffraction (XRD) was employed to study the epitaxial quality of the films. Fig. 4 shows the typical diffraction pattern from the θ–2θ scan for a film annealed at 1000 °C. Only (h00) peaks of Eu$_2$O$_3$ and LAO are observed, suggesting that the Eu$_2$O$_3$ film is single phase with a preferential a-axis orientation. The full width at half-maximum (FWHM) of the rocking curve from the (400) reflection of Eu$_2$O$_3$ is about 0.8°. Fig. 4 also shows the ϕ scans on Eu$_2$O$_3$ {440} and LAO {110}. The 45° shift between Eu$_2$O$_3$ 440 and LAO {110} suggests a rotation of 45° between these two lattices.

Transmission electron microscopy (TEM) and selected area diffraction (SAD) were performed on a cross-sectional sample of Eu$_2$O$_3$ on LAO (100) which was annealed at 1000 °C. Fig. 5 shows a low-magnification bright-field TEM image of Eu$_2$O$_3$
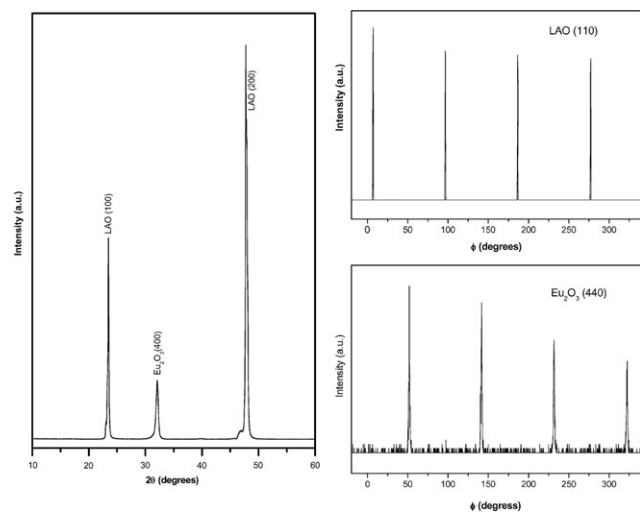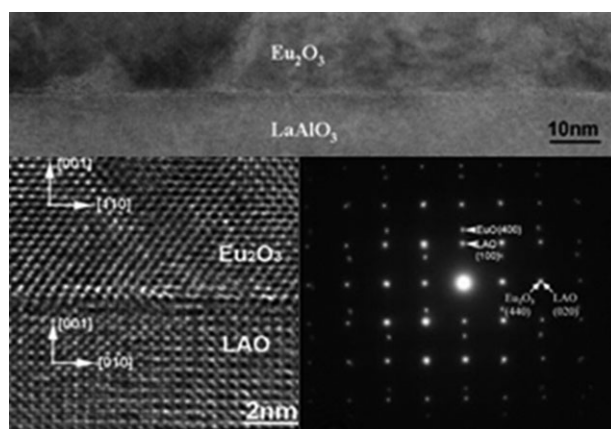

Fig. 5 Cross-sectional TEM images from Eu$_2$O$_3$ on LaAlO$_3$ substrate: (top) low-magnification image; (bottom right) corresponding SAD pattern from Eu$_2$O$_3$ and LaAlO$_3$; (bottom left) high-resolution image showing the interface between Eu$_2$O$_3$ and LaAlO$_3$.

with the beam along the [110] zone. It is clear that the interface is flat and without any visible secondary phases. The Eu$_2$O$_3$ film has a relatively uniform contrast with no obvious columnar grain growth observed. The corresponding SAD pattern at the interface area was also taken from the same zone axis to confirm the orientation relations between the film and the substrate, as shown in Fig. 5. Diffraction dots from Eu$_2$O$_3$ are sharp and distinguishable, indicating the high quality of the film. This epitaxial relationship is not unreasonable considering the lattice parameter of bulk Eu$_2$O$_3$ ($\sim$10.86 Å, cubic structure) is about $2\sqrt{2}$ times that of LAO ($\sim$3.78 Å, cubic structure). A 45° rotation in the basal plane should appear between the substrate and the Eu$_2$O$_3$ film (Fig. 6).

With appropriate lattice matching PAD has produced epitaxial films of transition metal, lanthanide and actinide metal oxides. In addition to the production of high density films, the films can also be prepared without cracking. PAD results in crack-free films up to 300 nm thick. This is a convenient improvement for chemical techniques, given that a layer thickness of 200 nm or less is generally needed to avoid cracks in the conventional sol–gel-processed films. One of the explanations for microcrack formation in sol–gel-derived films is the condensation reaction and pore collapse in gel films under heat treatment.[18] In the PAD process the depolymerisation of the polymer results in a bottom-up growth process, where there is no stressing of the film prior to densification.[14]
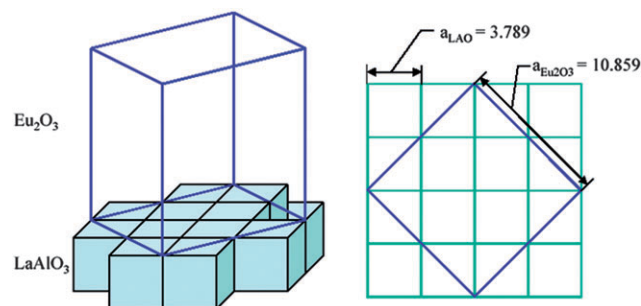

Fig. 4 XRD patterns of the Eu$_2$O$_3$ film on a LAO substrate: (a) θ–2θ scan; (b) ϕ-scans from (440) reflections of Eu$_2$O$_3$ film and the (110) of the LAO substrate.

Fig. 6 Lattice relationship between Eu$_2$O$_3$ and LaAlO$_3$.

Stoichiometry control

One of the key aspects of any method for the formation of metal oxide films is control over stoichiometry and dopant levels. PAD makes the development of mixed oxides extremely simple. The metal concentrations of the precursor solutions are determined by inductively coupled plasma atomic emission spectroscopy (ICP-AES).[14] With accurate concentrations known for the different metal systems, all that is required is to mix the solutions together in the required ratio. The mixture is then coated onto the substrate and thermally annealed. A clear example of this control is demonstrated by the formation of $Ba_{1-x}Sr_xTiO_3$ (BST) thin films with different Ba/Sr ratios ($x = 0.1–0.9$; interval of 0.1).[19]

The separate barium, strontium and titanium solutions are mixed accordingly to the final stoichiometry desired for the BST by adjusting the Ba, Sr and Ti ratios. The resulting solutions are spin coated on to LAO substrates. The thermal treatment is then performed in oxygen. Samples are then annealed by heating at 1000 °C for 1 h to induce crystallization. X-Ray diffraction (XRD) and transmission electron microscopy (TEM) analysis shows that all the BST films are epitaxial (see Fig. 7). Only $(00l)$ peaks of BST and LAO are observed in the XRD θ–2θ scans, suggesting that all the BST films are single phase with a preferential c-axis orientation (see Fig. 8). The full widths at half maximum (FWHMs) of rocking curves from the (002) reflections of BST films are in the range of 0.4–0.6°. The ϕ scans confirmed the epitaxial nature of the films.

All of the films show nonlinear dielectric behaviour with the applied electric field. Fig. 9 shows the zero-field dielectric constant (ε_0) (top) and tunability (bottom) [$(\varepsilon_0 - \varepsilon_E)/\varepsilon_0$, where ε_E is the dielectric constant at an applied field E] vs. x. The dielectric values of the films are comparable to the reported values of the films grown by pulsed laser deposition (PLD),[20] demonstrating the good quality of the BST films grown by PAD. In addition, the change of the dielectric properties of the BST films with the variation in the x values is also very similar to the BST films grown by PLD.[20]
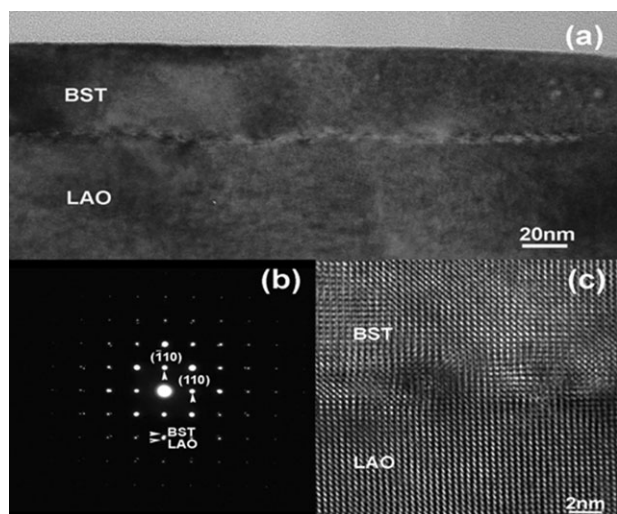

Fig. 7 TEM (top), HRTEM (bottom right) and SAD (bottom left) of $Ba_{0.5}Sr_{0.5}TiO_3$.

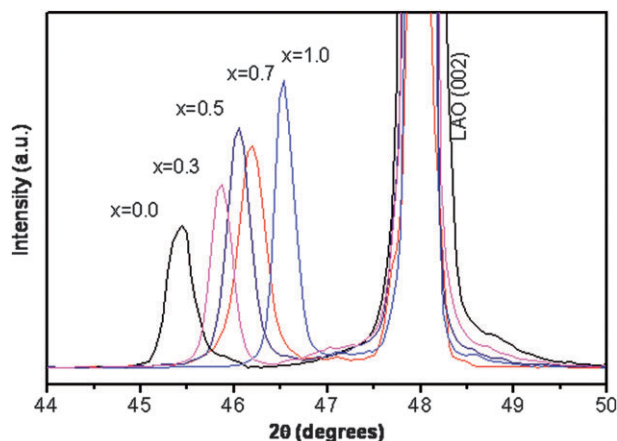**Fig. 8** XRD θ–2θ scans of the $Ba_xSr_{1-x}TiO_3$ films ($x = 0$, 0.3, 0.5, 0.7, 1.0).

Ferromagnetic $SrRuO_3$ thin films prepared epitaxially on LAO substrates using PAD have demonstrated a room-temperature resistivity of 300 $\mu\Omega$ cm^{-1}.[21] Spontaneous magnetization below 160 K indicates that the SRO film undergoes a ferromagnetic–paramagnetic phase transition at this temperature, as seen in Fig. 10. The spontaneous magnetization near the transition temperature follows the scaling law, $M \sim (T_c - T)^\alpha$, with an α value of 0.45 for the field parallel to the substrate surface.

Multilayered structures

The ability of any technique to achieve multilayer structures and devices is critical to its utility. PAD is compatible with the deposition of multiple layered devices. We have prepared films with a large magnetoresistance near room temperature using multilayer-coated $La_{0.67}Sr_{0.33}MnO_3/La_{0.67}Ca_{0.33}MnO_3$ (LSMO/LCMO) films using PAD.[22] The LSMO and LCMO compounds have similar lattice parameters and have a Curie temperature above and below room temperature, respectively, which makes them very attractive for preparing multilayers. We prepared multilayer-coated films by holding the LSMO : LCMO volume ratio constant (60 : 40) and changing the
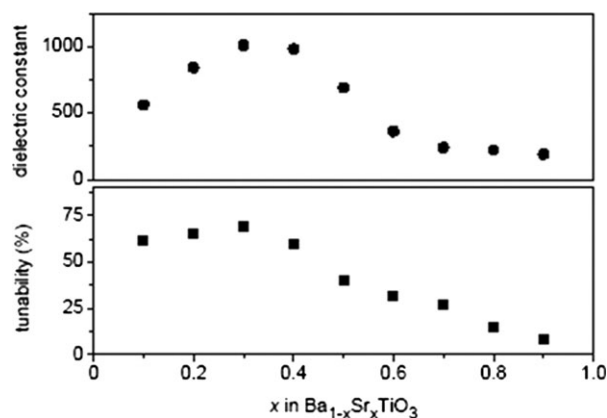

Fig. 9 (Top) Zero-field dielectric constant (ε_0) and (bottom) tunability [$(\varepsilon_0 - \varepsilon_E)/\varepsilon_0$, where ε_E is the dielectric constant at an applied field E] vs. x.
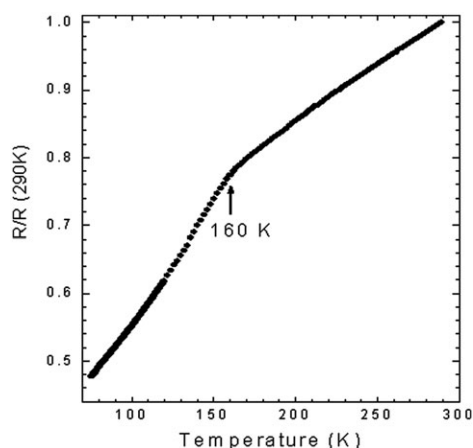
Fig. 10 The typical temperature dependence of the normalized resistance R/R(290 K) for a SRO film annealed at 550 °C at zero field.

number and the thickness of the individual layers. Details of the layered configuration with their sample identifications (ML1 and ML2) are illustrated in Fig. 11. To make a direct comparison of the multilayer-coated films, a single-phase film of $La_{0.67}Sr_{0.198}Ca_{0.132}MnO_3$ (LSCMO), which is a uniformly mixed phase of the LSMO/LCMO at a volume ratio of 60 : 40, was also prepared under similar conditions.

The single-phase $La_{0.67}Sr_{0.198}Ca_{0.132}MnO_3$ film shows a maximum MR of −58% at 280 K. On the other hand, a much larger MR near room temperature is achieved using layered structures. These results clearly indicate that the transition temperature (or temperature of maximum MR) and the magnitude of the MR can be manipulated through multilayer coating of two ferromagnetic materials. Similar properties could not be achieved by simply mixing LSMO with LCMO phases at the same volume ratio.[22]

Lattice engineering

One of the great advantages of heteroepitaxy is the ability to direct crystal phase using the lattice matching of the substrate. Careful choice of the lattice can impart sufficient influence to provide a major barrier to interconversion of crystalline forms
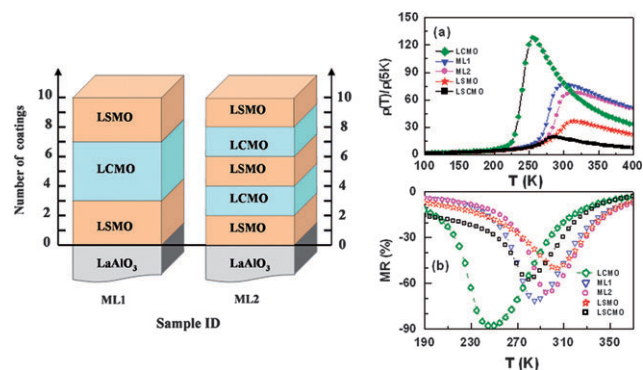

Fig. 11 The left panel shows the sample identification. Right: (a) normalized resistivity as a function of temperature for the multilayer-coated LSMO/LCMO films (ML1 and ML2) along with that of the pure LSMO, LCMO and LSCMO films; and (b) the temperature dependent magnetoresistance (at 5 T) for different films.
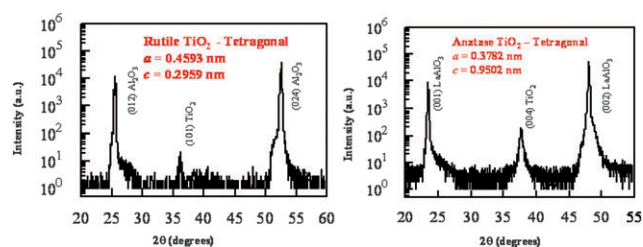

Fig. 12 X-Ray diffraction spectra: θ–2θ scans of rutile (left) TiO_2 films deposited by PAD on R-cut sapphire and θ–2θ scans of epitaxial anatase (right) TiO_2 films deposited by PAD on $LaAlO_3$.

even preventing access to the thermodynamic phase of any given material. This is best demonstrated in the TiO_2 system where rutile (the thermodynamic phase) and anatase (a low-temperature phase) both have tetragonal unit cells, but their lattice parameters (rutile: $a = 4.593$ Å and $c = 2.959$ Å; anatase: $a = 3.782$ Å and $c = 9.502$ Å), space groups, and atomic positions in the unit cells are different from one another. Using PAD we have prepared both rutile and anatase TiO_2 from the same precursor solutions.[14] The X-ray diffraction (XRD) 2θ-scan of the TiO_2 film on R-cut sapphire ($a = 5.364$ Å and $c = 13.11$ Å), annealed at 1100 °C, is shown in Fig. 12 (left). The film has a rutile structure and is preferentially oriented out of the plane. Epitaxial anatase TiO_2, in contrast, may be obtained on pseudocubic $LaAlO_3$ ($a = 3.789$ Å). Fig. 12 (right) is the XRD 2θ-scan of the film annealed at 980 °C, showing the anatase structure and its preferentially out-of-the-plane orientation. The epitaxial nature of anatase TiO_2 on $LaAlO_3$ is evidenced by the ϕ-scans of (101) TiO_2 and (101) $LaAlO_3$ (not shown).

Oxidation state control by lattice engineering

Epitaxial films, whose crystallographic order is controlled by that of the substrate or heteroepitaxy, is relatively common. However, when we consider how convenient this process is, it is somewhat surprising that heteroepitaxy has not been employed to direct and control the oxidation state of the thin film. Materials with easily variable oxidation states should be controlled by the lattice engineering as easily as crystal form is directed by the lattice. This turns out to be the case when PAD is employed to produce epitaxial films of uranium oxides. Uranium oxide films have been extensively studied for many years, but no examples of epitaxial films have been reported. The PAD technique is a "bottom-up" growth methodology and therefore the influence of the lattice is emphasised to the extreme. This is most clearly demonstrated when PAD solutions of UO_2^{2+} are coated onto LAO, c-sapphire or r-sapphire. Not only does the lattice control the crystal form of the oxide produced, during thermal treatment, but also the oxidation state of the material obtained. Thus, LAO produces epitaxial UO_2 films, whereas the same conditions result in orthorhombic or hexagonal U_3O_8 on R- and c-plane sapphire, respectively.[23] Fig. 13 shows the epitaxial relationships between the UO_2 and the $LaAlO_3$ (LAO) substrate being $(100)UO_2||(100)LAO$ and $\langle 110 \rangle UO_2||\langle 010 \rangle LAO$. In addition the cross-sectional high-resolution electron microscopy (HRTEM) image taken along the [100] $LaAlO_3$ zone axis is

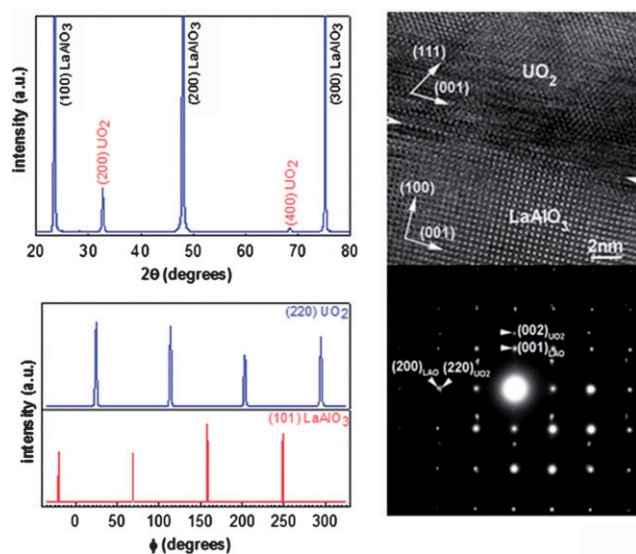Fig. 13 θ–2θ scans of UO_2 films deposited on a single crystal (100) $LaAlO_3$ substrate (left upper); ϕ-scans of the (220) epitaxial UO_2 films and the (101) $LaAlO_3$ (left lower). The HRTEM (right upper) and the selected-area electron diffraction pattern (right lower) of the UO_2 attest to the quality of the film.

Fig. 14 SEM of uncoated (left) and ZrO_2 coated (right) anodisc™.

shown. The HRTEM image shows a very sharp interface between the UO_2 film and the $LaAlO_3$ substrate. There are no detectable second phases and no voids in the film. The selected-area electron diffraction pattern displays sharp diffraction dots on the diffraction patterns further confirming that the UO_2 film is of high quality epitaxy.

The samples prepared on sapphire were obtained with the exact same solution and thermal treatment as the UO_2. However, the lattice match for the sapphires drives the uranium to form U_3O_8. After extensive X-ray and HRTEM analysis it was determined that epitaxial U_3O_8 obtained on the c-plane sapphire has a hexagonal structure with lattice parameters of $a = 0.6815$ nm and $c = 0.4144$ nm. In contrast, the R-plane sapphire substrate results in orthorhombic U_3O_8.

This is a unique example of lattice pinning of metal oxide oxidation states. The stability of these films is remarkable. Even after being exposed to air at room temperature for more than 400 days or at 275 °C in air for 10 days, we observed no change in the diffraction patterns.[23] Clearly, lattice engineering provides a strong driving force for oxidation state control.

Coating nanostructures

We have observed example after example of how PAD is a "bottom-up" assembly method for the formation of metal oxides. This is largely due to the "soup" of metal-coordinated polymer that is present until the last instances of the thermal treatment. This metal polymer coating is attracted to the substrate as the polymer evaporates. This process has a significant advantage over other techniques because it allows for conformal coating of complex/porous 3-D structures.

Most techniques such as sputtering, PLD or molecular beam epitaxy (MBE) are line-of-sight processes that severely limit their ability to evenly coat nanoscale features with high aspect ratios. Although chemical vapor deposition (CVD) is
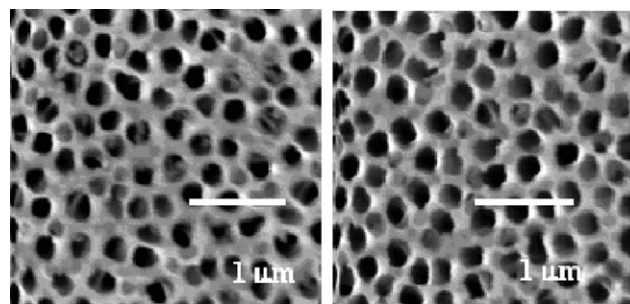
not restricted to line-of-sight coating it has many of the same issues in coating high aspect ratio nanoscale features because material flowing through the vapour phase must encounter a surface and react to form a film. This results in build-up of the film where the vapour phase first contacts the surface and results in clogging at the entrance to very small pores as opposed to a smooth coating throughout the interior of the pore. Sol–gel is a solution based technique that will readily enter all of the pore surfaces in a material, but the resulting films are far from conformal. In sol–gel the metal oxide film is formed *via* a metal oligomerization that occurs in the bulk solution. This process leads to internal clogging of narrow features as film formation can nucleate and grow within the bulk solution instead of at the surface. The thermal treatment during the PAD process causes the metal polymer to attract to the surface before oxide growth, therefore nanofeatures are coated evenly without obscuring or blocking the features. Coatings of even deep nanofeature substrates such as commercial anodisc™ membranes, which are typically 60 μm thick, can be simply achieved using PAD.[24] Fig. 14 shows a commercial anodisc™ membrane before and after coating with ZrO_2 using PAD. The pores on the membrane were conformally coated with 20 nm of ZrO_2. There was no significant change in the membrane performance as determined by both gas and solution flow rate measurements. However, the effect on the chemical stability of the membrane was significant. The uncoated and ZrO_2-coated membranes were placed in a pH 12.4 solution. The Anodiscs™ coated with ZrO_2 lasted for 24 h whereas the uncoated samples were destroyed after 15 min.

Conclusions

The successful growth of both simple and complex metal oxides by PAD suggests that PAD is a useful alternative to the growth of high-quality metal oxide films. Composition control is straightforward and with lattice pinning of oxidation states, access to new oxide compositions is now possible. The key features in PAD are the depolymerisation of the polymer and the protection of the metal until the last moments of deposition when the oxide film is formed. This delayed assembly results in efficient mixing of the metals and high density films. In addition this bottom-up growth method provides a unique capability in conformal coating of nanofeatures.

References

1 A. Elshabini-Riad and F. D. Barlow III, *Thin Film Technology Handbook*, McGraw-Hill, New York, 1998.
2 D. L. Smith, *Thin Film Deposition*, McGraw-Hill, New York, 1995.
3 F. F. Lange, *Science*, 1996, **273**, 903–909.
4 L. L. Hench and J. K. West, *Chem. Rev.*, 1990, **90**, 33–72.
5 D. C. Bradley, *Chem. Rev.*, 1989, **89**, 1317–22.
6 C. J. Brinker and G. W. Scherer, *Sol–Gel Science: The Physics and Chemistry of Sol–Gel Processing*, Academic Press, Inc., San Diego, CA, 1990.
7 T. P. Niesen and M. R. De Guire, *J. Electroceram.*, 2001, **6**, 169–207.
8 J. Emerson-Reynolds, *J. Chem. Soc., Trans*, 1884, **45**, 162.
9 R. S. Mane and C. D. Lokhande, *Mater. Chem. Phys.*, 2000, **65**, 1, and references therein.
10 Y. F. Nicolau, *Appl. Surf. Sci.*, 1985, **22**, 1061–1074.
11 M. Ristov, G. J. Sinadinovski and I. Grozdanov, *Thin Solid Films*, 1985, **123**, 63–67.
12 H. M. Pathan and C. D. Lokhande, *Bull. Mater. Sci.*, 2004, **27**, 85–111.
13 K. C. Lee and J. G. Hwu, *J. Vac. Sci. Technol., A*, 1998, **16**, 2641–2645.
14 Q. X. Jia, T. M. McCleskey, A. K. Burrell, Y. Lin, G. E. Collis, H. Wang, A. D. Q. Li and S. R. Foltyn, *Nat. Mater.*, 2004, **3**, 529–532.
15 I. E. Kirillina, V. N. Voronov, A. M. Dolgonosov and M. A. Lazeikina, *Teploenergetika*, 1988, 74–75.
16 H. M. Luo, M. Jain, T. M. McCleskey, E. Bauer, A. K. Burrell and Q. X. Jia, *Adv. Mater.*, 2007, **19**, 3604–3607.
17 Y. Lin, H. Wang, H. E. Hawley, S. R. Foltyn, Q. X. Jia, G. E. Collis, A. K. Burrell and T. M. McCleskey, *Appl. Phys. Lett.*, 2004, **85**, 3426–3428.
18 H. Kozuka, M. Kajimura, T. Hirano and K. Katayama, *J. Sol–Gel Sci. Technol.*, 2000, **19**, 205–209.
19 Y. Lin, J.-H. Lee, H. Wang, Y. Li, S. R. Foltyn, Q. X. Jia, G. E. Collis, A. K. Burrell, T. M. McCleskey and T. M, *Appl. Phys. Lett.*, 2004, **85**, 5007–5009.
20 Y. Gim, T. Hudson, Y. Fan, C. Kwon, A. T. Findikoglu, B. J. Gibbons, B. H. Park and Q. X. Jia, *Appl. Phys. Lett.*, 2000, **77**, 1200.
21 H. M. Luo, M. Jain, S. A. Baily, T. M. McCleskey, A. K. Burrell, E. Bauer, R. F. DePaula, P. C. Dowden, L. Civale and Q. X. Jia, *J. Phys. Chem. B*, 2007, **111**, 7497–7500.
22 M. Jain, P. Shukla, Y. Li, M. F. Hundley, H. Wang, S. R. Foltyn, A. K. Burrell, T. M. McCleskey and Q. X. Jia, *Adv. Mater.*, 2006, **18**, 2695–2698.
23 A. K. Burrell, T. M. McCleskey, P. Shukla, H. Wang, T. Durakiewicz, D. P. Moore, C. G. Olson, J. J. Joyce and Q. X. Jia, *Adv. Mater.*, 2007, **19**, 3559–3563.
24 P. Shukla, E. M. Minogue, T. M. McCleskey, Q. X. Jia, Y. Lin, P. Lu and A. K. Burrell, *Chem. Commun.*, 2006, 847–849.